

Comparison between Tensor Networks and Variational Quantum Classifier

G. Laskaris,^{1,2} Ar. A. Melnikov,¹ M. R. Perelshtein,¹ R. Brasher,¹ T. Bäck,² and F. Neukart^{1,2}

¹*Terra Quantum AG, Kornhausstrasse 25, 9000 St. Gallen, Switzerland*

²*LIACS, Leiden University Leiden, Netherlands*

The primary objective of this paper is to conduct a comparative analysis between two Machine Learning approaches: Tensor Networks (TN) and Variational Quantum Classifiers (VQC). While both approaches share similarities in their representation of the Hilbert space using a logarithmic number of parameters, they diverge in the manifolds they cover. Thus, the aim is to evaluate and compare the expressibility and trainability of these approaches. By conducting this comparison, we can gain insights into potential areas where quantum advantage may be found. Our findings indicate that VQC exhibits advantages in terms of speed and accuracy when dealing with data, characterized by a small number of features. However, for high-dimensional data, TN surpasses VQC in overall classification accuracy. We believe that this disparity is primarily attributed to challenges encountered during the training of quantum circuits. We want to stress that in this article, we focus on only one particular task and do not conduct thorough averaging of the results. Consequently, we recommend considering the results of this article as a unique case without excessive generalization.

I. INTRODUCTION

A quantum computer encodes information in quantum states and utilizes different quantum mechanical properties, such as superposition, entanglement, and interference to execute calculations [1–4]. Quantum machine learning (QML) is machine learning implemented in a quantum computer or a quantum simulator. QML can be realized, for example, by parameterized quantum circuits (PQC). A specific flavor of PQC that we discuss in this paper is variational quantum classifiers (VQC). VQC models are PQC which are optimized using classical optimization algorithms to find the optimal value of the parameters [5].

Related to QML techniques are quantum-inspired algorithms such as tensor network (TN) models [6–8]. Typically, the way that VQC and TN operate, are similar. Their main difference is the way they manipulate the weights of the model (see Sec. III). TN utilizes the TT-decomposition to manipulate efficiently the high-dimensional tensors that represent the weights of the model and the features of the data. The parameters that consist the weights tensor of TN are optimized using the Riemannian optimization algorithm [9–11].

In this work, we apply VQC and TN to publicly available datasets to compare the performance of models. We are following up on research where the performance of the TN model was compared to that of standard gradient descent (SGD) in classification tasks [11]. There, the superiority of the TN model over SGD was shown for different datasets.

Among the many applications of the models used in this paper are applications of QML [12–14] and quantum-inspired tensor networks [15] in high-energy physics. Moreover, applications in image classification [16–18] can be used in autonomous systems of self-driving cars and unmanned aerial vehicles [19]. The need for powerful computations is evident in these applications since they require decision-making in real-time, along with

fast adaptation to the environment. Those applications strongly indicate that QML produces impressive results in comparison to classical models.

In general, QML is a promising candidate for solving demanding tasks in various fields. For example, in drug discovery, it is proven that QML techniques, such as generative adversarial networks (GAN) and convolutional neural networks (CNN) are superior to their classical analog [20–22].

The main goal of this article is to give a more solid understanding of different ML models. Specifically, we investigate the respective strengths and weaknesses of a variational quantum classifier and a tensor network model.

This article is structured as follows. In Sec. II we provide a short introduction to all necessary preliminaries to grasp the essence of this research. The preliminaries include a brief introduction to machine learning, in Sec. II A, and tensor networks, in Sec. II B. There, important techniques will be introduced, namely principal component analysis (PCA) [23], Variational circuits [24, 25], Matrix Product States (MPS) [25–28], Riemannian Optimization [9, 10], tensor train decomposition (TT-decomposition) [11, 29], for the implementation of the models. Additionally, in Sec. III, we explain the architectures of the models, how we used the aforementioned techniques in the models, and how we implemented the VQC (in Sec. III A) and TN (in Sec. III B) models in general. Furthermore, in Sec. IV we present the experimental results and discuss the performance of both models under a common denominator. Finally, in Sec. V, we discuss the trade-offs between the models on binary classification tasks. Moreover, in the same section, we refer to potential future work and also strengthen our results by verifying the experiments.

II. PRELIMINARIES

A. Quantum Machine learning

QML can be characterized as the combination of classical ML with quantum mechanics to some extent. The quantum mechanical element can be inserted through different means. Some examples are the implementation of quantum data as qubits, the use of a parameterized quantum circuit (PQC) [30], for the training of the model, or even quantum algorithms such as Quantum Approximate Optimization Algorithm (QAOA) [31], Variational Quantum Eigensolver (VQE) [32] or Quantum Support Vector Machines (QSVM) [33], for the further improvement of the model training and optimization [34].

A specific application of PQC is the variational quantum classifier (VQC) [24, 30]. The VQC is composed of two different parts, the encoder part, and the variational part [30]. In the encoder, a quantum circuit is utilized to encode the features of samples into qubits. It is obvious that there are many different encoding techniques, such as angle encoding, amplitude encoding, wave-function encoding, and others [30, 35]. The choice of encoding is closely related to different kernel methods. These methods are used to project the data into a higher-dimensional feature space, where the same problem is typically easier to solve. So, the proper choice of feature space is paramount for the solution of the problem.

For example, non-linear feature maps [36, 37] are capable to project data into a feature space where their relative distance is much different. In that way, it is possible that the samples can be easier distinguished from one another, and thus a binary classification among them can be achieved accurately. The inner product of two points (samples) in the feature space characterizes the kernel similarity function [38].

The second component of a VQC is the variational or parameterized part, which is a quantum circuit of a given ansatz. It generally consists of entangling layers and rotation gates on the qubits, with free, tunable parameters. The main hyper-parameter of this model is the number of variational layers chosen for the variational architecture. In order to give some depth to the variational circuit, which is crucial for its performance, we have to repeat the structure of *CNOT* gates and rotations multiple times. Finally, measurements on one or more qubits are made, so the model can make predictions after observing the output states.

B. Tensor networks

A tensor network can be described as the diagrammatic representation of a collection of tensors [39]. Tensor networks are usually used in many-body quantum systems [40, 41], and one of the most well-studied families of tensor networks are matrix product states or MPS [27, 42].

An MPS or a tensor-train (TT) is a 1-dimensional state of a tensor network, where tensors are connected through one index called bond index (the dimension of which is called a virtual dimension or **tensor train-rank** [39]) and have another index called visible index, sticking out of the tensor (the dimension of which is called the physical dimension [39]) (Fig. 1). In general, the TT-rank r can vary from bond index to bond index and is regarded as a hyper-parameter of the model.

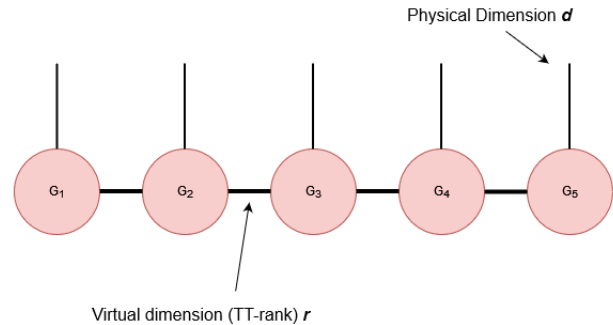


FIG. 1: MPS example with five tensors $G_i, i \in \{1, 2, \dots, 5\}$, a common TT-rank $r_1 = r_2 = \dots = r_4 = r$ and a common physical dimension $d_1 = d_2 = \dots = d_5 = d$.

After applying the TT-decomposition [11, 29] method on a tensor \mathcal{A} (Fig. 2), the resulting network has the structure of an open boundary condition MPS. TT-decomposition is a way of manipulating multi-dimensional tensors without suffering from the curse of dimensionality [29]. In the heart of TT-decomposition lies the singular value decomposition (SVD) [29, 43, 44], which is applied $d-1$ times on the desired d -dimensional tensor \mathcal{A} , in order to get the d tensors (TT-cores), which can efficiently represent \mathcal{A} .

The general idea of TT-decomposition is to approximate all entries of the tensor \mathcal{A} by the product of d matrices $G_k(i_k)$ which belong on G_k TT-cores of dimension $r_k \times r_{k-1}$ (with $r_0 = r_d = 1$ since we want the product to return a scalar value), within an error ϵ . The indices i_k , with $k \in \{1, 2, \dots, d\}$ and $i_k \in \{1, 2, \dots, n_k\}$, represent the dimension which enumerates over the k -th index of tensor \mathcal{A} , where n_k is the dimension of the k -th index of \mathcal{A} . More specifically, we have

$$A_{i_1 i_2 \dots i_d} = \prod_{k=1}^d G_k(i_k) \quad (1)$$

In order to train a tensor \mathcal{B} to approximate the tensor \mathcal{A} through TT-decomposition, we need a proper optimizer. A suitable optimizer for this task is the Riemannian optimization algorithm [11, 29].

Riemannian geometry is a branch of differential geometry that includes and describes the Riemannian manifolds. Manifolds are topological spaces that locally re-

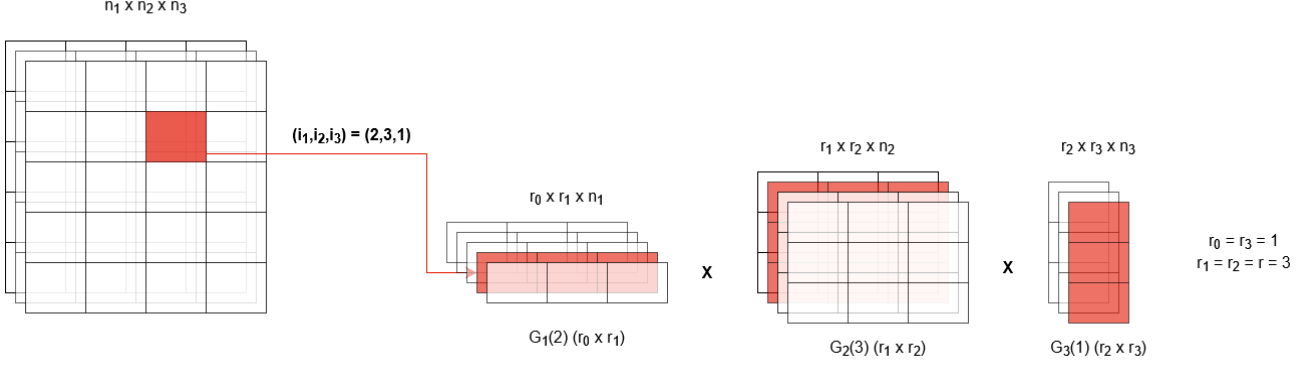


FIG. 2: TT-decomposition example of a three-dimensional tensor of which the entry $\mathcal{A}_{2,3,1}$ is calculated. A fixed rank $r = 3$ is used for all TT-cores $G_k(i_k)$, where $k \in \{1, 2, 3\}$ and i_k is the respective index of the desired entry. So, in order to calculate the entry $\mathcal{A}_{2,3,1}$, we need to multiply the second matrix from the first TT-core (this corresponds to the first coordinate of the entry), with the third matrix of the second TT-core (which corresponds to the second coordinate of the entry) and finally multiply with the first matrix of the final TT-core (which corresponds to the third coordinate of the entry).

semble Euclidean spaces [10]. A Riemannian manifold \mathcal{M} is a smooth Hausdorff and second countable manifold (by smooth we mean it is C^∞ , infinitely times differentiable), equipped with a positive-definite smoothly varying inner product g metric, which can be used to determine an inner product on each point p of the tangent space $T_p\mathcal{M}$ of \mathcal{M} [9, 11].

In a given d -dimensional tensor \mathcal{A} , we can apply the TT-decomposition with a fixed rank $r_i = r$, $i \in \{1, 2, \dots, d-1\}$ and of course $r_0 = r_d = 1$. All such tensors like \mathcal{A} , belong to a Riemannian manifold

$$\mathcal{M}_r = \{\mathcal{A} \in \mathbb{R}^{n_1 \times n_2 \times \dots \times n_d} : \text{TT-rank}(\mathcal{A}) = r\} \quad (2)$$

Consider tensors \mathcal{X} and \mathcal{W} , where \mathcal{X} is of rank 1 and consists of all the features that describe the data. \mathcal{W} can be considered as a d -dimensional tensor, which contains all tunable weights of the model. As we show, the dimensions of \mathcal{W} can be $n_1 = n_2 = \dots = n_d = 2$ and thus its entries are in $\mathbb{R}^{2 \times 2 \times \dots \times 2}$. That is because the interactions of the features of the data can be multiplied with the weights according to the following equation:

$$\hat{y}(\mathbf{x}) = \sum_{i_1=0}^1 \sum_{i_2=0}^1 \dots \sum_{i_d=0}^1 \mathcal{W}_{i_1 i_2 \dots i_d} \prod_{j=1}^d x_j^{i_j} \quad (3)$$

Here $\hat{y}(\mathbf{x})$ represents the prediction of the model [11]. In other words, that prediction is the product of the relative weight with the features. When an entry of the weight tensor is multiplied with some features, then the relative indices of the weight tensor become 1, and the remaining become 0.

For a two-dimensional example

$$\hat{y}(\mathbf{x}) = \mathcal{W}_{00} + \mathcal{W}_{10}x_1 + \mathcal{W}_{01}x_2 + \mathcal{W}_{11}x_1x_2 \quad (4)$$

we see that for indices $i_1 = i_2 = 0$ we get $x_1^0 = x_2^0 = 1$, for $i_1 = 1, i_2 = 0$, we get $x_1^1 = x_1, x_2^0 = 1$, and so on.

Riemannian optimization attempts to minimize the following loss function

$$L(\mathcal{W}) = \sum_{s=1}^N \text{MSE}(\hat{y}(\mathbf{x}^{(s)}), y^{(s)}) + \frac{\lambda}{2} \|\mathcal{W}\|_F \quad (5)$$

where the term $\frac{\lambda}{2} \|\mathcal{W}\|_F$ is the L_2 regularization term, with λ being the regularization parameter and $\|\mathcal{W}\|_F$ the Frobenius norm of the weight tensor [45]. The $\text{MSE}(\hat{y}(\mathbf{x}^{(s)}), y^{(s)}) : \mathbb{R}^2 \rightarrow \mathbb{R}$ is the mean squared error or the squared loss of the predictions $\hat{y}(\mathbf{x}^{(s)})$ towards true values $y^{(s)}$, and the s refers to the current sample examined, with the total number of samples in the data being N .

Applying the Riemannian optimization algorithm on \mathcal{W} we can fine-tune its entries in such a way that the model can make accurate predictions. The steps of the Riemannian optimization algorithm we follow are the calculation of the gradient of the loss, with respect to \mathcal{W} . Then, project it to the tangent space of \mathcal{M}_r . The projection at point \mathcal{W} which is $T_{\mathcal{W}}\mathcal{M}_r$. We define the projection as

$$\mathcal{P} = P_{T_{\mathcal{W}}\mathcal{M}_r} \left(\frac{\partial L}{\partial \mathcal{W}} \right) \quad (6)$$

Following the direction of the projection \mathcal{P} with a small learning step α we get out of \mathcal{M}_r and onto the tangent space $T_{\mathcal{W}}\mathcal{M}_r$. As a consequence, there is an increase in the TT-rank. To return to \mathcal{M}_r , we need to reduce (rounding [29]) the TT-rank back to r . This reduction can be achieved by retracting the projection from point

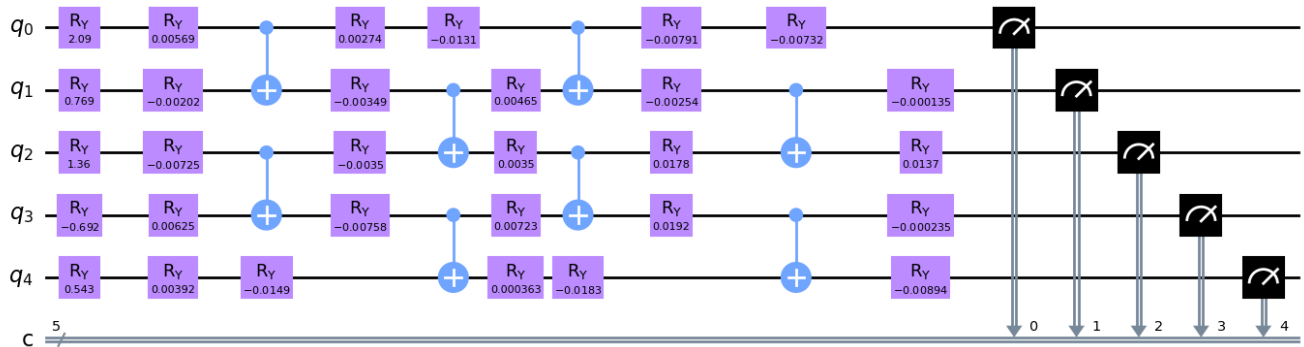


FIG. 3: Example of the architecture used for the VQC model, with 5 qubits and 2 variational layers.

\mathcal{W} , by a small learning step α . In total, we take a step $\mathcal{W} - \alpha \mathcal{P}$ in order to return back to the manifold.

By recursively applying those steps, one can minimize the loss, and as a result, tune \mathcal{W} to minimize the $L(\mathcal{W})$.

III. IMPLEMENTATION

We compare the performance on a binary classification task between a Variational Quantum Classifier (VQC) and a Tensor Network (TN) with Riemannian optimization. We applied both models on the UCI car dataset of 2013 [46].

The dataset has 1728 samples with six categorical features each. Converting the categorical features to binary with one-hot encoding we end up with 21 binary features in total. For the experiments, we used a random splitting of the data, with a splitting ratio of 80% between training and validation sets. Additionally, for the data pre-processing we used PCA, so we were able to run experiments with 2, 5, 10 and 16 principal components of the data, as well as all 21 features.

The dataset originally was a multi-class classification problem, with classes (unacc, acc, good, vgood), which refers to the acceptability of each car in the dataset. In order to convert it to a binary classification problem, we merged all three classes (acc, good, vgood) into one class (namely "acc") which consists 29% of the data, we later represented this class with +1, and the other class ("unacc") with -1 which consists the 71% of the data. The dataset can be characterized as unbalanced and thus the choice of accuracy as a metric might be incorrect. However, after extended experimentation, both accuracy and F1-score, which is an excellent metric for imbalanced datasets, reported almost the same results. The features of the dataset consist of the buying price, price of maintenance, number of doors, number of people to carry, size of luggage boot, and estimated safety of the car.

We initialize both models with random weights and used the validation accuracy as a comparison metric between them.

A. Variational Quantum Classifier model

For the implementation of the encoding part of VQC, we used the cosine/sine encoding [47, 48]. For this encoding, we start from an all $|0\rangle$ state and we apply R_y single qubit rotations on every qubit. After the encoding part, each qubit would be in the state

$$|0\rangle \rightarrow R_y |0\rangle = \cos\left(\frac{\pi}{2}x_k\right) |0\rangle + \sin\left(\frac{\pi}{2}x_k\right) |1\rangle \quad (7)$$

where $k \in \{1, 2, \dots, N\}$ and N is the total number of features/qubits used for each sample. In that way, we introduce and pass information from the data to the quantum circuit.

After the encoding part, we have to establish a variational architecture. We chose to follow the Noisy Intermediate Scale Quantum (NISQ) friendly architecture used in [25]. The main hyper-parameter here is the number of variational layers used. Each layer consists of $CNOT$ gates with control on all odd-numbered qubits, then a layer of R_y rotations applied on each individual qubit, $CNOT$ gates with control on every even-numbered qubit, and one more R_y layer on every qubit. In total, every layer needs to train $2N$ parameters (plus N for the 0-th layer, which consists of only an R_y rotation layer on every qubit). Thus, $N(2L + 1)$ parameters need to be tuned, where L is the number of layers used.

In Fig. 3 an example of the architecture of the VQC model is illustrated. This example refers to a five-qubit model with two variational layers. At the end of the circuit, we utilize only the first measurement for the prediction. If the expectation value of the measurement falls under the predefined threshold, we classify the sample to the -1 ("unacc") class, otherwise, we classify it to the +1 ("acc") class. The threshold we use throughout all the experiments is set to 0.5.

The MSE has been used as a loss function for VQC and for the circuit implementation PennyLane (version = 0.30.0) library has been used [49]. For the optimizer, we

tried Standard Gradient Descent (SGD), Nesterov momentum optimizer [50], and Adaptive Momentum optimizer (Adam) [51, 52]. Adam returned the best results, so we chose that for all the experiments with VQC. During training, a batch size of 32 samples was used, along with a decaying learning rate with an initial value of 0.1 and a decay rate of 0.95.

B. Tensor Network model

For the Tensor Network model (TN), we followed the implementation used in [11]. In this model, the method of TT-decomposition has been applied in order to manipulate the weights tensor in a more efficient way, especially when working with high-dimensional data. Polynomial encoding as defined in (8) has been used as data encoding.

$$\mathcal{X}_{i_1 i_2 \dots i_d} = \prod_{k=1}^d x_k^{i_k} \quad (8)$$

where, $\mathcal{X}_{i_1 i_2 \dots i_d}$ represents the tensor which includes the features of the samples, and $x_k^{i_k}$ is the k -th feature of the sample. For the values i_j , the indices $j \in \{1, 2, \dots, d\}$ and $i_j \in \{0, 1\}$. Thus, for the feature of a sample, it will be

$$x_j^{i_j} = \begin{cases} 1 & , \text{if } i_j = 0 \\ x_j & , \text{if } i_j = 1 \end{cases}$$

This model is trained with Riemannian optimization and uses the logistic loss as a loss function. Its main hyper-parameter is the TT-rank used for the TT-decomposition. The total number of parameters that need to be trained in this model is $2Nr^2$, where N is the number of features used, and r is the TT-rank. We notice that the number of parameters in the TN model scales much faster in comparison with VQC since the TN parameters scale quadratically with the rank.

For the implementation of the TN model, the `ttpy` library, which is a python implementation of the TT-Toolbox library [53], has been used, in coordination with other libraries with mathematical tools, such as `numpy` [54] and `scikit-learn` [55].

As mentioned above, the predictor of this model is based on the simple linear product between the features tensor \mathcal{X} and the weights tensor \mathcal{W} . So in total, we can rephrase equation (3) as

$$\hat{y}(\mathbf{x}) = \langle \mathcal{X}, \mathcal{W} \rangle \quad (9)$$

There is no need for a separate bias term since this is integrated in \mathcal{W} as $\mathcal{W}_{00\dots 0}$.

IV. RESULTS

We compare the VQC and TN models with different numbers of qubits and principal components. In order to decide which number of principal components we will run experiments for, we compose a scree plot analysis [56] in Fig. 4.

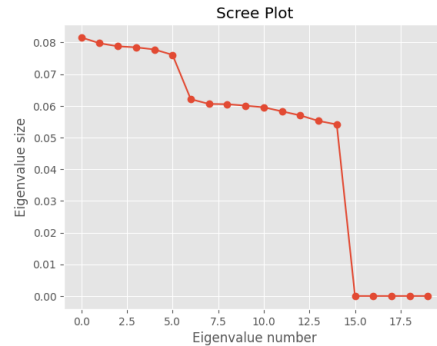


FIG. 4: Scree plot analysis for up to 20 principal components. The eigenvalue number represents the principal components, and the eigenvalue size represents the percentage of the original data that each principal component expresses. The plot represents the 1st principal component with 0.0 and so on.

Each point in Fig. 4 represents the percentage that is going to be added to the total expressibility of the dataset. As a result, it is logical to make experiments with 2 qubits, which seem to give low expressibility, 5 qubits which are again in low expressibility but still have to add to the overall eigenvalue size, 10 qubits which are in the mid-range of the eigenvalue size contribution, and 16 qubits which in principle add almost 0% to a model with 15 principle components.

In Fig. 6, we show the results of a binary classification experiment on the UCI car dataset using a VQC in comparison to a TN model as described above. In both experiments, we used different numbers of principal components from the car dataset and recorded their accuracy with the number of variational layers/TT-ranks and the number of principal components used in training. As a result, it seems that for the tested dataset and model architectures, the TN model increases its performance significantly as the number of principal components increases. Additionally, VQC also increases its performance and achieves better classification, however with more principal components, the training time, and thus the effort for parameter optimization in the variational layer increases significantly and often leads to local minima or vanishing gradients.

In Fig. 5b, we show the respective plot of the validation accuracy with the number of trainable parameters, for 5 qubits. It is evident that VQC performs better than TN. As the trainable parameters increase, notice that the performance of TN converges, in contrast with VQC

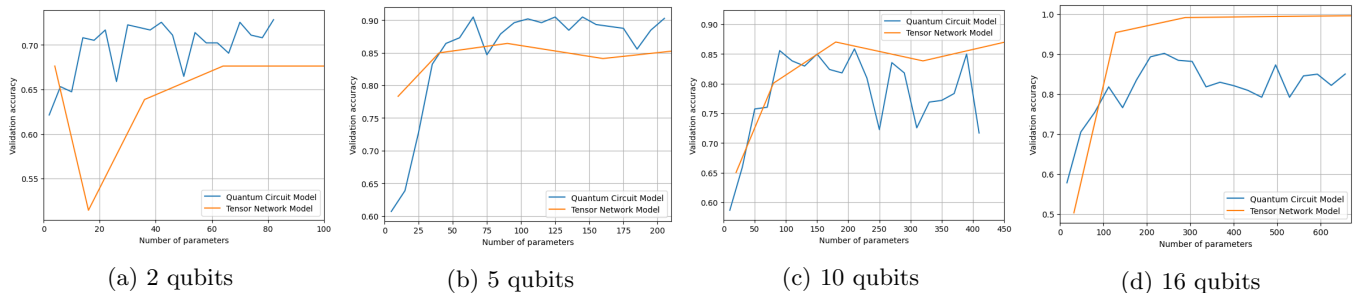


FIG. 5: The validation accuracy achieved by TN and VQC models with dependency on the number of trainable parameters.

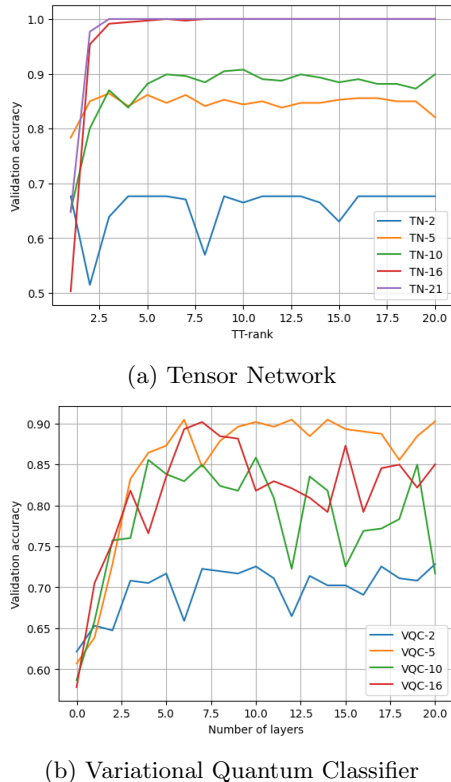


FIG. 6: Plot of the validation accuracy for the two models with the number of TT-rank/variational layers, for different numbers of principal components/qubits (2, 5, 10, 16)

which oscillates around 90% but always above TN.

In Fig. 5c we compare the 10 qubits TN and VQC. Notice that TN surpasses VQC considering it achieves better accuracy than VQC for ≥ 150 trainable parameters. TN performance in 10 qubits seems comparable with the 5 qubits VQC. However, the experiments with more than 10 qubits, indicate that TN is the dominant model for high-dimensional binary classification tasks. This observation is based on the poor trainability of VQC for a large number of qubits.

For 16 qubits in Fig. 5d, TN is clearly better than

VQC, regarding the validation accuracy. TN manages to achieve perfect classification and VQC shows a more stable behavior in comparison with the 10 qubit experiment. Under 100 parameters, VQC surpasses TN, which is not the case for more than 100 parameters.

V. DISCUSSION

We are not able to claim that one model is better than the other. Accuracy depends on the available computational power and time. Also, the dimensionality of the data plays a significant role when we want to choose between the models. If the only consideration is the overall accuracy, then TN models might be a better choice, especially, if the problem involves high-dimensional data, to give a perspective, data with more than 10 – 15 features. TT-decomposition enables us to manipulate the high-dimensional weight tensor much faster than other methods. Riemannian optimization seems to be an excellent fit as an optimizer to TN since it outperforms SGD [11] and assists TN in achieving better classification. A drawback of TN is that requires significantly more trainable parameters compared to VQC.

On the other hand, VQC equipped with a dimensionality reduction technique (such as PCA), or used on a problem with low-dimensional data, might be a better choice than TN. For example, 5 qubits VQC can reach $\sim 91\%$ validation accuracy on the UCI car dataset. We observed that VQC achieved maximum accuracy after a small number of epochs. This is especially promising to reduce the training time of VQCs with a larger number of qubits.

There are indications that VQC can achieve even better accuracy with more qubits. As shown in Fig. 6b with 16 qubits, it is capable of outperforming the 5 qubits for 6 – 8 layers. So with hyper-parameter tuning or more training, VQC might also be suitable for high-dimensional data. However, because training time for the 16 qubits VQC requires much computation time, we did not investigate this possibility as much as it seems to deserve.

Overall, by examining the plots, we notice that VQC is

consistently the model that achieves the best validation accuracy for a small number of variational layers or low

TT-rank. This result strengthens our previous finding about VQC, being the preferable method when we need to train a model within a limited time frame.

-
- [1] Roman Rietsche, Christian Dremel, Samuel Bosch, Léa Steinacker, Miriam Meckel, and Jan-Marco Leimeister. Quantum computing. *Electronic Markets*, pages 1–12, 2022.
- [2] Michael A. Nielsen and Isaac L. Chuang. *Quantum Computation and Quantum Information: 10th Anniversary Edition*. Cambridge University Press, USA, 10th edition, 2011.
- [3] Andreas Bayerstadler, Guillaume Becquin, Julia Binder, Thierry Botter, Hans Ehm, Thomas Ehmer, Marvin Erdmann, Norbert Gaus, Philipp Harbach, Maximilian Hess, et al. Industry quantum computing applications. *EPJ Quantum Technology*, 8(1):25, 2021.
- [4] Alexey Pyrkov, Alex Aliper, Dmitry Bezrukov, Yen-Chu Lin, Daniil Polykovskiy, Petrina Kamyra, Feng Ren, and Alex Zhavoronkov. Quantum computing for near-term applications in generative chemistry and drug discovery. *Drug Discovery Today*, page 103675, 2023.
- [5] Marco Cerezo, Andrew Arrasmith, Ryan Babbush, Simon C Benjamin, Suguru Endo, Keisuke Fujii, Jarrod R McClean, Kosuke Mitarai, Xiao Yuan, Lukasz Cincio, et al. Variational quantum algorithms. *Nature Reviews Physics*, 3(9):625–644, 2021.
- [6] Artem A Melnikov, Alena A Termanova, Sergey V Dolgov, Florian Neukart, and Michael Perelshtein. Quantum state preparation using tensor networks. *Quantum Science and Technology*, 2023.
- [7] Zheng-Zhi Sun, Cheng Peng, Ding Liu, Shi-Ju Ran, and Gang Su. Generative tensor network classification model for supervised machine learning. *Physical Review B*, 101(7):075135, 2020.
- [8] Jun Qi, Chao-Han Huck Yang, and Pin-Yu Chen. Qtn-vqc: An end-to-end learning framework for quantum neural networks. *arXiv preprint arXiv:2110.03861*, 2021.
- [9] Gary Bécigneul and Octavian-Eugen Ganea. Riemannian adaptive optimization methods. *arXiv preprint arXiv:1810.00760*, 2018.
- [10] John M Lee. *Riemannian manifolds: an introduction to curvature*, volume 176. Springer Science & Business Media, 2006.
- [11] Alexander Novikov, Mikhail Trofimov, and Ivan Oseledets. Exponential machines. *arXiv preprint arXiv:1605.03795*, 2016.
- [12] Wen Guan, Gabriel Perdue, Arthur Pesah, Maria Schuld, Koji Terashi, Sofia Vallecorsa, and Jean-Roch Vlimant. Quantum machine learning in high energy physics. *Machine Learning: Science and Technology*, 2(1):011003, 2021.
- [13] Kapil K Sharma. Quantum machine learning and its supremacy in high energy physics. *Modern Physics Letters A*, 36(02):2030024, 2021.
- [14] Alessio Gianelle, Patrick Koppenburg, Donatella Lucchesi, Davide Nicotra, Eduardo Rodrigues, Lorenzo Sestini, Jacco de Vries, and Davide Zuliani. Quantum machine learning for b -jet charge identification. *arXiv preprint arXiv:2202.13943*, 2022.
- [15] Timo Felser, Marco Trenti, Lorenzo Sestini, Alessio Gianelle, Davide Zuliani, Donatella Lucchesi, and Simone Montangero. Quantum-inspired machine learning on high-energy physics data. *npj Quantum Information*, 7(1):111, 2021.
- [16] Arsenii Senokosov, Alexander Sedykh, Asel Sagingalieva, and Alexey Melnikov. Quantum machine learning for image classification. *arXiv preprint arXiv:2304.09224*, 2023.
- [17] Yunqian Wang, Yufeng Wang, Chao Chen, Runcai Jiang, and Wei Huang. Development of variational quantum deep neural networks for image recognition. *Neurocomputing*, 501:566–582, 2022.
- [18] Rui Huang, Xiaoqing Tan, and Qingshan Xu. Variational quantum tensor networks classifiers. *Neurocomputing*, 452:89–98, 2021.
- [19] Qingyuan Song, Wen Wang, Weiping Fu, Yuan Sun, Denggui Wang, and Zhiqiang Gao. Research on quantum cognition in autonomous driving. *Scientific reports*, 12(1):300, 2022.
- [20] Junde Li, Mahabubul Alam, M Sha Congzhou, Jian Wang, Nikolay V Dokholyan, and Swaroop Ghosh. Drug discovery approaches using quantum machine learning. In *2021 58th ACM/IEEE Design Automation Conference (DAC)*, pages 1356–1359. IEEE, 2021.
- [21] Alexey Pyrkov, Alex Aliper, Dmitry Bezrukov, Yen-Chu Lin, Daniil Polykovskiy, Petrina Kamyra, Feng Ren, and Alex Zhavoronkov. Quantum computing for near-term applications in generative chemistry and drug discovery. *Drug Discovery Today*, page 103675, 2023.
- [22] Maria Avramouli, Ilias K Savvas, Anna Vasilaki, and Georgia Garani. Unlocking the potential of quantum machine learning to advance drug discovery. *Electronics*, 12(11):2402, 2023.
- [23] Sidharth Prasad Mishra, Uttam Sarkar, Subhash Taphder, Sanjay Datta, D Swain, Reshma Saikhom, Sasmita Panda, and Menalsh Laishram. Multivariate statistical data analysis-principal component analysis (pca). *International Journal of Livestock Research*, 7(5):60–78, 2017.
- [24] Elies M Gil Fuster. Variational quantum classifier. 2019.
- [25] Artem A Melnikov, Alena A Termanova, Sergey V Dolgov, Florian Neukart, and Michael Perelshtein. Quantum state preparation using tensor networks. *Quantum Science and Technology*, 2023.
- [26] Frank Verstraete, Diego Porras, and J Ignacio Cirac. Density matrix renormalization group and periodic boundary conditions: A quantum information perspective. *Physical review letters*, 93(22):227205, 2004.
- [27] David Perez-Garcia, Frank Verstraete, Michael M Wolf, and J Ignacio Cirac. Matrix product state representations. *arXiv preprint quant-ph/0608197*, 2006.
- [28] Yiqing Zhou, E Miles Stoudenmire, and Xavier Waintal. What limits the simulation of quantum computers? *Physical Review X*, 10(4):041038, 2020.
- [29] Ivan V Oseledets. Tensor-train decomposition. *SIAM*

- Journal on Scientific Computing*, 33(5):2295–2317, 2011.
- [30] Marcello Benedetti, Erika Lloyd, Stefan Sack, and Mattia Fiorentini. Parameterized quantum circuits as machine learning models. *Quantum Science and Technology*, 4(4):043001, 2019.
- [31] Edward Farhi, Jeffrey Goldstone, and Sam Gutmann. A quantum approximate optimization algorithm. *arXiv preprint arXiv:1411.4028*, 2014.
- [32] Jules Tilly, Hongxiang Chen, Shuxiang Cao, Dario Picozzi, Kanav Setia, Ying Li, Edward Grant, Leonard Wossnig, Ivan Rungger, George H Booth, et al. The variational quantum eigensolver: a review of methods and best practices. *Physics Reports*, 986:1–128, 2022.
- [33] Rui Zhang, Jian Wang, Nan Jiang, and Zichen Wang. Quantum support vector machine without iteration. *Information Sciences*, 635:25–41, 2023.
- [34] M Cerezo, Guillaume Verdon, Hsin-Yuan Huang, Lukasz Cincio, and Patrick J Coles. Challenges and opportunities in quantum machine learning. *Nature Computational Science*, 2(9):567–576, 2022.
- [35] Ryan LaRose and Brian Coyle. Robust data encodings for quantum classifiers. *Physical Review A*, 102(3):032420, 2020.
- [36] Dimitrios Athanasakis, John Shawe-Taylor, and Delmiro Fernandez-Reyes. Learning non-linear feature maps. *arXiv preprint arXiv:1311.5636*, 2013.
- [37] Aaron Baughman, Kavitha Yogaraj, Raja Hebbar, Sudeep Ghosh, Rukhsan Ul Haq, and Yoshika Chhabra. Study of feature importance for quantum machine learning models. *arXiv preprint arXiv:2202.11204*, 2022.
- [38] Alberto Di Meglio Elías F. Combarro, Samuel González-Castillo. *A Practical Guide to Quantum Machine Learning and Quantum Optimization*. Packt Publishing, 2023.
- [39] Jacob C Bridgeman and Christopher T Chubb. Hand-waving and interpretive dance: an introductory course on tensor networks. *Journal of physics A: Mathematical and theoretical*, 50(22):223001, 2017.
- [40] Simone Montangero, Evenson Montangero, and Evenson. *Introduction to tensor network methods*. Springer, 2018.
- [41] Glen Evenbly and Guifré Vidal. Tensor network states and geometry. *Journal of Statistical Physics*, 145:891–918, 2011.
- [42] Román Orús. A practical introduction to tensor networks: Matrix product states and projected entangled pair states. *Annals of physics*, 349:117–158, 2014.
- [43] Steven L Brunton and J Nathan Kutz. *Data-driven science and engineering: Machine learning, dynamical systems, and control*. Cambridge University Press, 2022.
- [44] Tamara G Kolda and Brett W Bader. Tensor decompositions and applications. *SIAM review*, 51(3):455–500, 2009.
- [45] Liqun Qi, Shenglong Hu, Xinzhen Zhang, and Yannan Chen. Tensor norm, cubic power and gelfand limit. *arXiv preprint arXiv:1909.10942*, 2019.
- [46] Marko Bohanec. Car Evaluation. UCI Machine Learning Repository, 1997. DOI:<https://doi.org/10.24432/C5JP48>.
- [47] E Miles Stoudenmire and David J Schwab. Supervised learning with quantum-inspired tensor networks. arXiv 2016. *arXiv preprint arXiv:1605.05775*.
- [48] Samuel Yen-Chi Chen, Chih-Min Huang, Chia-Wei Hsing, and Ying-Jer Kao. Hybrid quantum-classical classifier based on tensor network and variational quantum circuit. *arXiv preprint arXiv:2011.14651*, 2020.
- [49] Ville Bergholm, Josh Izaac, Maria Schuld, Christian Gogolin, Shah Nawaz Ahmed, Vishnu Ajith, M. Sohaib Alam, Guillermo Alonso-Linaje, B. Akash Narayanan, Ali Asadi, Juan Miguel Arrazola, Utkarsh Azad, Sam Banning, Carsten Blank, Thomas R Bromley, Benjamin A. Cordier, Jack Ceroni, Alain Delgado, Olivia Di Matteo, Amintor Dusko, Tanya Garg, Diego Guala, Anthony Hayes, Ryan Hill, Aroosa Ijaz, Theodor Isaacson, David Ittah, Soran Jahangiri, Prateek Jain, Edward Jiang, Ankit Khandelwal, Korbinian Kottmann, Robert A. Lang, Christina Lee, Thomas Loke, Angus Lowe, Keri McKiernan, Johannes Jakob Meyer, J. A. Montañez-Barrera, Romain Moyard, Zeyue Niu, Lee James O’Riordan, Steven Oud, Ashish Panigrahi, Chae-Yeun Park, Daniel Polatajko, Nicolás Quesada, Chase Roberts, Nahum Sá, Isidor Schoch, Borun Shi, Shuli Shu, Sukin Sim, Arshpreet Singh, Ingrid Strandberg, Jay Soni, Antal Száva, Slimane Thabet, Rodrigo A. Vargas-Hernández, Trevor Vincent, Nicola Vitucci, Maurice Weber, David Wierichs, Roeland Wiersema, Moritz Willmann, Vincent Wong, Shaoming Zhang, and Nathan Killoran. PennyLane: Automatic differentiation of hybrid quantum-classical computations, 2022.
- [50] Goran Nakerst, John Brennan, and Masudul Haque. Gradient descent with momentum—to accelerate or to super-accelerate? *arXiv preprint arXiv:2001.06472*, 2020.
- [51] Diederik P Kingma and Jimmy Ba. Adam: A method for stochastic optimization. *arXiv preprint arXiv:1412.6980*, 2014.
- [52] Agnes Lydia and Sagayaraj Francis. Adagrad—an optimizer for stochastic gradient descent. *Int. J. Inf. Comput. Sci.*, 6(5):566–568, 2019.
- [53] Ivan Oseledets. Tt-toolbox. <https://github.com/oseledets/TT-Toolbox>, 2023. Retrieved June 16, 2023.
- [54] Charles R. Harris, K. Jarrod Millman, Stéfan J. van der Walt, Ralf Gommers, Pauli Virtanen, David Cournapeau, Eric Wieser, Julian Taylor, Sebastian Berg, Nathaniel J. Smith, Robert Kern, Matti Picus, Stephan Hoyer, Marten H. van Kerkwijk, Matthew Brett, Allan Haldane, Jaime Fernández del Río, Mark Wiebe, Pearu Peterson, Pierre Gérard-Marchant, Kevin Sheppard, Tyler Reddy, Warren Weckesser, Hameer Abbasi, Christoph Gohlke, and Travis E. Oliphant. Array programming with NumPy. *Nature*, 585(7825):357–362, September 2020.
- [55] F. Pedregosa, G. Varoquaux, A. Gramfort, V. Michel, B. Thirion, O. Grisel, M. Blondel, P. Prettenhofer, R. Weiss, V. Dubourg, J. Vanderplas, A. Passos, D. Cournapeau, M. Brucher, M. Perrot, and E. Duchesnay. Scikit-learn: Machine learning in Python. *Journal of Machine Learning Research*, 12:2825–2830, 2011.
- [56] Gibbs Y Kanyongo. Determining the correct number of components to extract from a principal components analysis: a monte carlo study of the accuracy of the scree plot. *Journal of modern applied statistical methods*, 4(1):13, 2005.